Journal of Structural Biology **128,** 3–14 (1999)
Article ID jsbi.1999.4172, available online at http://www.idealibrary.com on IDEAL®

Review: Electron Crystallography: Present Excitement, a Nod to the Past, Anticipating the Future

Robert M. Glaeser

Department of Molecular and Cell Biology and Lawrence Berkeley National Laboratory, University of California Berkeley, Berkeley, California 94720

Received May 11, 1999, and in revised form August 2, 1999

From a modest beginning with negatively stained samples of the helical T4 bacteriophage tail, electron crystallography has emerged as a powerful tool in structural biology. High-resolution density maps, interpretable in terms of an atomic structure, can be obtained from specimens prepared as well-ordered, two-dimensional crystals, and the resolution achieved with helical specimens and icosahedral viruses is approaching the same goal. A hybrid approach to determining the molecular structure of complex biological assemblies is generating great interest, in which high-resolution structures that have been determined for individual protein components are fitted into a lower resolution envelope of the large complex. With this as background, how much more can be anticipated for the future? Considerable scope still remains to improve the quality of electron microscope images. Automation of data acquisition and data processing, together with the emergence of computational speeds of 10^{12} floating point operations per second or higher, will make it possible to extend high-resolution structure determination into the realm of single-particle microscopy. As a result, computational alignment of single particles, i.e., the formation of "virtual crystals," can begin to replace biochemical crystallization. Since single-particle microscopy may remain limited to "large" structures of 200 to 300 kDa or more, however, smaller proteins will continue to be studied as helical assemblies or as two-dimensional crystals. The further development of electron crystallography is thus likely to turn increasingly to the use of single particles and small regions of ordered assemblies, emphasizing more and more the potential for faster, higher throughput.

INTRODUCTION

The development of a crystallographic perspective within biological electron microscopy, incorporating concepts of three-dimensional density maps and associated Fourier mathematics, can be traced to the work of DeRosier and Klug (1968) on the helical structure of the T4 bacteriophage tail. To be sure, other biological work with a significantly crystallographic perspective preceded this milestone paper, including high-resolution electron diffraction experiments on fibers (Parsons and Martius, 1964) and the application of optical diffraction to electron microscope images (Klug and Berger, 1964), or was under concurrent development (Hoppe *et al.,* 1968; Glaeser and Thomas, 1969; Labaw and Rossmann, 1969). Still, the seminal paper of DeRosier and Klug, far more influentially than any other, marks the beginning of a program of three-dimensional structure determination of biological macromolecules that is based upon electron, rather than X-ray, scattering. Electron crystallography of biological macromolecules, broadly defined, has now expanded to encompass a range of specimens and experimental approaches that was hardly imaginable 30 years ago. First icosahedral viruses (Crowther *et al.,* 1970a) and then two-dimensional crystals (Matricardi *et al.,* 1972; Taylor and Glaeser, 1974; Unwin and Henderson, 1975) were added as specimens suitable for structure determination by electron microscopy.

The use of a naturally crystalline membrane protein, bacteriorhodopsin, was a key factor in the development of methods to take electron crystallography to ever increasing resolution, resulting ultimately in an atomic model (Henderson *et al.,* 1990). This pioneering work has been followed in turn by the determination of the structure of LHC II, a photosynthetic light-harvesting protein (Kuhlbrandt *et al.,* 1994); an independent redetermination of bacteriorhodopsin structure at higher resolution (Kimura *et al.,* 1997); and crystallographic refinement of the original structure of bacteriorhodopsin (Grigorieff *et al.,* 1996).

Even more ambitiously, three-dimensional reconstruction of large macromolecular structures such as the mammalian fatty acid synthetase complex (Hoppe *et al.,* 1974) and the ribosome (Knauer *et al.,* 1983;

1047-8477/99 $30.00

Oettl *et al.,* 1983) were carried out from complete (tomographic) tilt series on individual particles. Recognizing the limitations of radiation damage, however, the use of single particles was soon improved by the introduction of methods to merge data from many identical particles (Frank, 1975; Saxton and Frank, 1977; van Heel and Frank, 1981; Frank and van Heel, 1982). A comprehensive description of the subsequent development of these single-particle methods and their application to a wide variety of biological structures can be found in the book by Frank (1996). The discovery that thin, aqueous films can be vitrified by rapid freezing (Dubochet *et al.,* 1982; Lepault *et al.,* 1983; Dubochet *et al.,* 1988) was also a vital advance in single-particle microscopy. Thus, the combination of (1) merging data from images recorded with effectively "no radiation damage" and (2) the preservation of native structure in frozen-hydrated specimens provides the essential background for determining high-resolution structures from images of single particles.

It is the most recent advances in each of these areas, however, and not the historical development summarized above, that has begun to draw the attention of the broader community of structural biologists. The structure of tubulin, a protein that is central to many functions in eukaryotic cells, has recently been solved through the use of two-dimensional crystals (Nogales *et al.,* 1998). This success has drawn considerable notice because of its impact on cell biology and because of the fact that crystals suitable for X-ray crystallography have not been available. Increasing improvements in resolution are also being made with tubular (helical) crystals of the nicotinic acetylcholine receptor (Miyazawa *et al.,* 1999) and the Ca-ATPase ion pump (Zhang *et al.,* 1998). In both cases, basic elements of secondary structure are already visible, and completion of atomic structures seems inevitable. The resolution achieved with icosahedral viruses has also become sufficient to recognize four-helix bundles within the density map (Bottcher *et al.,* 1997; Conway *et al.,* 1997). The resolution of single-particle reconstructions of the ribosome has improved to well below 2 nm (Malhotra *et al.,* 1998), and an insightful theoretical analysis of single-particle imaging has shown that there is almost no physical barrier to reaching atomic resolution by merging data from large numbers of individual particles (Henderson, 1995). At the same time, the field of structural biology has come to recognize the power of a hybrid approach in which atomic models of component proteins, determined by X-ray crystallography, NMR spectroscopy, or high-resolution electron microscopy, are fitted with unexpected precision into the lower resolution envelope of complex, functional assemblies (Rayment *et al.,* 1993; Olson *et al.,* 1993; Agrawal *et al.,* 1998; Nogales *et al.,* 1999). These molecular envelopes can be obtained relatively easily by electron cryo-microscopy, whereas the prospect of solving the structure of ever-larger complexes by X-ray crystallography becomes increasingly daunting.

The work presented at the Granlibakken Symposium in December 1998, much of which is included in the papers in this issue, gives an excellent sense of the momentum of current work. The growing significance of electron crystallography within structural biology is illustrated by the number of new structures on which work is well advanced, such as aquaporin (Mitsuoka *et al.,* 1999), rhodopsin (Krebs *et al.,* 1998), gap junctions (Unger *et al.,* 1999), and monolayer crystals of α-actinin (Tang *et al.,* unpublished observations). Even more importantly, new methods of preparing ordered specimens continue to be developed, of which special mention is deserved for the formation of helical assemblies on tubular lipids (Wilson-Kubalek *et al.,* 1998) and the crystallization of detergent-solubilized membrane proteins on lipid monolayers (Levy *et al.,* 1999). The prospect of an even higher quality of electron microscope image data, which can be achieved through improved experimental protocols as well as through improved instrumentation, further fuels the growing enthusiasm now felt for electron crystallography.

The anticipated future articulated by Henderson (1995), and surely one of the motivations in the earliest development of the electron microscope, is that characterization of structures at atomic resolution will become routine through electron microscopy of isolated particles. Data from low-dose images of a very large number of single particles must be merged together, of course, in order to avoid structural changes that would occur due to radiation damage at high electron exposures. Computational alignment of images of single particles at atomic resolution results in the formation of "virtual crystals," producing a result that is equivalent to what would be obtained by the alignment of the particles themselves during biochemical crystallization. That such a powerful capability is even physically possible does not yet seem to have been adequately appreciated, however. It is the goal here to encourage a broader awareness of what physics will allow and in the process to identify some of the remaining milestones that engineering, growing computational speed, and human ingenuity must still achieve.

RADIATION DAMAGE PRECLUDES OBTAINING ATOMIC RESOLUTION IMAGES FROM INDIVIDUAL MOLECULES

Gabor, in the preface to a monograph by Marton (1968), recalled that his first response to the idea of

an electron microscope, probably like that of most physicists, was "Everything under the electron beam would burn to a cinder." Gabor was right, to be sure, but he could not anticipate, in 1928, the ingenuity that subsequently led to sample preparations that leave fossilized remains, which are remarkably accurate replicas of the original. Nor, without the invention of the modern computer, could he then speak of how much information would be extracted by averaging multiple copies of noisy images, which can be recorded before the destruction of the sample has gone too far (Glaeser, 1971; Glaeser *et al.,* 1971b; Unwin and Henderson, 1975; Kuo and Glaeser, 1975).

A quantitative physical analysis of elastic and inelastic scattering cross sections provides a definitive basis for understanding why biological molecules become fragmented beyond recognition, long before statistically well-defined images can be built up (Breedlove and Trammel, 1970). Quantitative measurement of the fading of electron diffraction intensities from model crystalline specimens at helium temperature (Glaeser *et al.,* 1971a) as well as at room temperature (Glaeser, 1971)—when combined with the Rose criterion for statistical definition of image features—added further, experimentally based weight to the same conclusion. The 70-year-old dream to take advantage of the short wavelength of high-energy electrons to image the atomic structure of individual protein molecules thus is, as Gabor correctly understood it, an impossible dream.

A more recent analysis of neutron scattering cross sections, on the other hand, just barely allows the imaging of individual molecules at atomic resolution—assuming a favorable isotopic substitution of sample materials (Henderson, 1995). In this case, however, the engineering solutions that are called for (enormous increases in neutron flux and the ability to focus neutrons at high resolution) also seem to make this possibility unachievable.

Quantitative estimations, both experimental and theoretical, thus require that many individual, statistically noisy images must be used in order to build up a final, high-resolution image (Glaeser, 1971; Glaeser *et al.,* 1971b). The idea, illustrated schematically in Fig. 1, is that the radiation dose that would severely fragment a single molecule can be distributed instead over many identical molecules. As a result, only a few molecules are fatally damaged, and the statistically well-defined image that is obtained by pooling data remains that of an undamaged molecule.

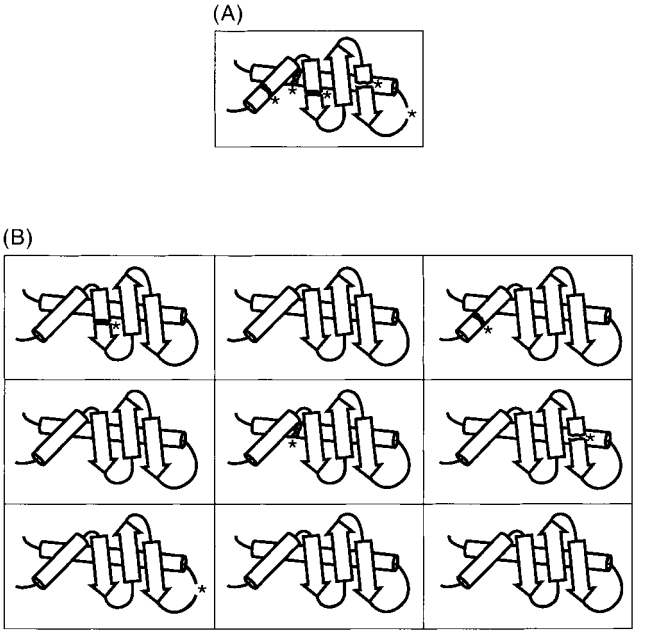

FIG. 1. A schematic cartoon that illustrates the fact that high-resolution images must use a large number of identical molecules. In (A) a single molecule has received too high an exposure, and as a result it is fragmented in five different places, indicated by the starred positions. In (B) the same exposure has been distributed over nine identical molecules. Only five of the nine molecules are damaged, and those that have been hit by a damaging event are not as severely fragmented as is the single molecule in (A). The image that is obtained by averaging over the molecules in (B) will thus be almost the same as that of an undamaged molecule.

WHAT IS THE MINIMUM NUMBER OF MOLECULES THAT IS REQUIRED TO OBTAIN A STATISTICALLY WELL-DEFINED, THREE-DIMENSIONAL DENSITY MAP AT 0.3-nm RESOLUTION?

The number of molecules from which data must be merged can be estimated in terms of just three quantities: the elastic scattering cross section, the maximum exposure that can be tolerated by a single molecule, and a suitable criterion for adequate statistical definition in the merged data (Henderson, 1995). Images of single molecules can themselves be invisible relative to the ambient shot noise (Caspar, 1975; Saxton and Frank, 1977), and still the data from many identical molecules can be merged to give a statistically well-defined, average image. The same principle applies to merging data in three dimensions and does so equally well for isolated molecules as it does for crystalline arrays.

Contrary to the intuition that many may first have on this point, the size of the molecule does not affect the number of molecules that must be used. Briefly, but noting that an alternative derivation is given by Henderson (1995), there is a minimum electron exposure that is required to image the three-dimensional position of a single atom. That exposure must be distributed over N_p particles, where

$$N_p = \frac{\text{exposure required for the image}}{\text{exposure that damages the molecule}}. \quad (1)$$

Since image formation is a linear process, in the weak phase approximation, the steps taken to image one atom in three dimensions will simultaneously image all atoms in their correct respective positions, regardless of the size of the object. This basic principle is inherent in the dose fractionation theorem in tomography (Hegerl and Hoppe, 1976; McEwen *et al.,* 1995).

Using values of $\sigma = 50$ pm^2 for the elastic scattering cross section for carbon (100 keV electrons), a maximum allowed electron exposure of 500 nm^{-2}, and the requirement that the intensity of the average Fourier coefficient of the structure should be three times the standard deviation of the shot noise, Henderson calculated that N_p must be greater than or equal to 12 600 molecules in order to obtain a three-dimensional density map at 0.3-nm resolution (Henderson, 1995).

Theoretically, an even smaller number of particles would be sufficient, however, as can be inferred by application of the dose fractionation theorem and the Rose (1948) criterion of statistical definition of image features. As is justified in the Appendix, the image of a single carbon atom can be modeled reasonably well as a disc of diameter 0.3 nm, whose intensity (contrast) is about 2% lower than that of the surrounding area. The Rose criterion states that such a disc can be reliably detected against a uniform background of shot noise if the exposure is

$$N_q = \frac{25}{d^2C^2} \cong 7 \times 10^5 \text{ electrons/nm}^2, \qquad (2)$$

where N_q is the number of quanta (here, electrons) per unit area; d is the diameter of the image disc; and C is the contrast. Essentially, the same required electron exposure is calculated by the equation used in Saxberg and Saxton (1981) for the value at which the image of an 0.3-nm feature would be three times the shot noise, if its mass density was 1 g/cm^3 (i.e., water). The density of protein ($\sim$1.3 g/cm^3) is only a little bit higher than this.

Assuming that the maximum electron exposure that can be tolerated by a single molecule is 500 nm^{-2}, the figure used by Henderson, the full exposure, $N_q = 7 \times 10^5$ electrons/nm^2, must be distributed over $N_p = 1400$ separate molecules, i.e., nine times fewer than the number estimated by Henderson (1995). The difference between these two estimates lies mainly in the criterion of "adequate statistical definition," since similar values are used for the scattering cross section and for the radiation damage limit (500 nm^{-2}). In the present estimate, it is required only that the coherent superposition of Fourier coefficients (producing the phase-contrast image of an atom) and not each individual structure factor (on average, of course) that must be statistically well defined. A smaller difference arises from the requirement for 5 standard deviations in the Rose equation, as opposed to the requirement of 3 standard deviations in Henderson's criterion.

The smaller, thus more "optimistic" estimate of the number of molecules needed to produce a high-resolution density map claims, in effect, that as few as one electron per "diffraction spot"—rather than 9, as required for Henderson's "3σ" criterion—is sufficient to produce a statistically well-defined image. Surprising as that claim may at first seem, the same conclusion is indicated by the earlier derivation by Henderson that the phase of a Fourier component of an image is accurate to 45° if just one electron is scattered into the corresponding diffraction spot (Henderson, 1992). A phase error of 45° corresponds, in turn, to the point at which a diffraction measurement just begins to add more to the signal than it does to the noise.

The actual number of particles that must be included in a real structure determination will, of course, be much larger than the minimum number that is calculated above. Many experimental factors can reduce the contrast of a single carbon atom to a value much smaller than the figure of 2% estimated above. In order to maintain the signal-to-noise at a level above the minimal criterion for detection, the number of particles must then be increased in proportion to the square of the contrast, assuming that shot noise is still the limiting factor. To illustrate this point, data must be merged from eight times more particles if the contrast is only 35% of the ideal value, while 100 times as many particles must be used if the contrast is only 10% of the ideal value, and even that is an optimistic estimate of the current situation.

Contrary to a common intuition, it is not necessary for the image of each atom in the structure to be statistically well defined in each projection image (Hegerl and Hoppe, 1976). Instead, the exposure needed to obtain a statistically well-defined image (of a single atom) in projection can be divided among an arbitrarily large number of different projections, which can themselves be distributed uniformly over all orientations of a molecule. As long as these many, statistically noisy images can be aligned, the data can be merged in three dimensions. As a result, the exposure needed to see each atom in three dimensions is precisely the same as the exposure needed to see a single atom in projection (Hegerl and Hoppe, 1976). The validity of this statement is independent of the size of the particle.

The number of projection views needed to obtain a three-dimensional reconstruction with isotropic resolution does depend upon the size of the particle, of

course. The number of projections must be at least $\pi D/d$, where D is the particle diameter and d is the resolution (Crowther *et al.,* 1970b). The dose fractionation theorem, and the alternative derivation of Henderson (1995), merely states that the required exposure can be distributed over as many different projection views as are required by the size of the particle. A given particle can, in principle, be used to record images in many different views, even though that is not what is normally done. As a result, the number of particles needed to generate a 3-D density map is independent of the particle size, although the number of required views does depend in an important way on the particle size.

WHAT IS THE SMALLEST MOLECULE FOR WHICH DATA CAN BE MERGED AT 0.3-nm RESOLUTION?

Henderson (1995) addressed this question in the context of an exhaustive, five-dimensional search covering the position (two dimensions) and orientation (three angles) of each particle. Following the concept of Saxton and Frank (1977), it is required that a particle be large enough to ensure that the value of the cross-correlation between the experimental image and the correct reference will be greater than the values that arise just by chance. Henderson's use of an exhaustive search over all alignments may represent too stringent (i.e., unnecessarily conservative) a criterion, in view of the fact that the alignment procedure would actually bootstrap progressively from lower to higher resolution, thereby drastically reducing the number of cross-correlation functions that need to be calculated. Even so, the value estimated in this way turns out to be surprisingly low, corresponding to a molecular mass of 38 kDa. The minimum particle size scales, however, as the square of the experimental contrast. In the present circumstances, in which the image contrast at high resolution is estimated to be only 10% of what it would be in a perfect image, the minimum particle size needed to merge the data to 0.3-nm resolution is estimated to be 4 MDa rather than 38 kDa.

An even smaller estimate of the minimum particle size is derived from the calculation of the image contrast for a single atom. We have previously estimated that $N_p = 1400$ carbon atoms would have to be superimposed in order for their combined image to be visible by the Rose criterion, if the exposure is limited to 500 nm^{-2}. The peak value of the cross-correlation function (but not, of course, its sharpness) will be the same (1) for two identical objects consisting of 1400 carbon atoms at a single point (a mathematical construct, of course) and (2) for two identical objects consisting of 1400 carbon atoms in a stereochemically reasonable, chemically bonded configuration. Considering the first of these two cases, the cross-correlation between two discs, each just detectable by the Rose criterion, would be well defined to a precision smaller than the size of the disc itself. By extrapolation, it seems likely that the same would also be true in the second case, i.e., for a molecular configuration of 1400 carbon atoms. According to this reasoning, then, even particles with a molecular mass equal to 12 Da $\times N_p \cong 17$ kDa, roughly half the size estimated by Henderson by a different criterion, could be aligned at 0.3-nm resolution. This estimate is based on only a plausibility argument, however, as it lacks the quantitative, statistical foundation employed by Henderson.

It is now more apparent than ever before that it is possible, in principle, to use images of individual particles, and not just crystals, to produce high-resolution structures of biological macromolecules. As estimated here, physics (but not current experimental practice; see below) would allow high-resolution image data to be merged together for any macromolecule (or domain of a macromolecule) larger than ~20 kDa, although a minimum of 1400 such images is needed to produce a three-dimensional structure, even in the ideal case. Averaging of a large set of images of individual particles can thus be seen as the end-game strategy for realizing the 70-year-old, semi-impossible dream to use individual protein molecules, rather than crystals, to determine their structure by electron microscopy.

The results currently achieved in practice, whether with single particles or with two-dimensional crystals, still fall well short of what physics says is possible, however. As an example, in order to obtain high-resolution projection maps of 2-D crystals one typically uses image fields containing 10^4 unit cells, and data are merged from at least 100 such crystals. Thus, it is clear that approximately 10^6 particles are needed for current work, rather than roughly 1000, or even 10 000, as estimated above. In addition, single-particle averaging can hardly be undertaken (currently) for particles smaller than 500 kDa, rather than 20 or 40 kDa. The explanation for the discrepancy between theory—as presented above—and current practice is certain to lie in the 10-fold loss of signal (Baldwin *et al.,* 1988; Henderson, 1992) that is characteristic of even the very best, contemporary images. As derived by Henderson (1995), the number of particles that must be merged in order to produce a 3-Å density map, and the minimum molecular weight required for particle alignment at this resolution, both scale as the inverse square of the "contrast" i.e., the actual signal relative to the signal that should, in principle, be there. Thus it must be expected that at least 100 times more particles are needed for images of the current quality than would

be required if the images were perfect representations of the object. By the same token, it must be expected that the minimum molecular mass required to successfully align particles at high resolution is currently at least 2 to 4 MDa, i.e., 100 times greater than would be the case for ideal images.

At a stage in which the high-resolution image contrast appears to be no more than 10% of what it theoretically should be, it would seem prudent to use a conservative estimate of the smallest particle size that is suitable for structural studies at high resolution. Thus, for the present, let us adopt Henderson's estimate that particle sizes may need to be at least 4 MDa in order to merge data to a resolution of 0.3 nm. This size limit may ultimately drop to ~250 kDa, assuming a potential improvement of contrast to 35% of the physical limit. These apparently large size limits nevertheless permit a wide scope for structural studies by electron crystallography. Single-particle electron microscopy should obviously be the method of choice for structural studies on large, complex assemblies, which become increasingly difficult for X-ray crystallography as the particle size increases. In addition, as mentioned before, high-resolution structures of individual protein components of such complexes will often have been determined in advance, further simplifying the task of visualizing the structure of the complex by electron microscopy.

Structural studies on smaller molecules will continue to require the use of methods to assemble them into two-dimensional crystals or helical arrays, of course. Segments of ordered assemblies need not be larger than a few tens of nanometers in size, however, since such segments soon become large enough to be processed as "single particles." On this size scale, problems of bending (always present in long helixes), wrinkling (a very severe problem for two-dimensional crystals), and even structural variation within larger crystalline fields (Frank *et al.,* 1988) can be dealt with inherently, as part of the alignment in five dimensions.

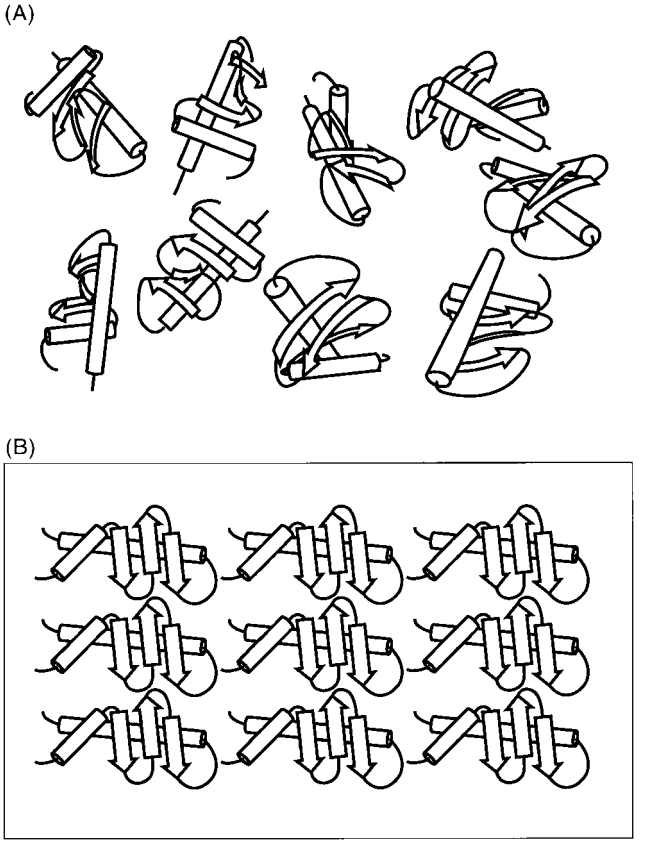

FIG. 2. A schematic cartoon that illustrates the role of crystals in crystallography. The ensemble of molecules in a crystal is already prealigned, thereby reducing the computational effort needed to superimpose the "invisible micrographs" (Caspar, 1975) that are obtained under low-dose conditions. In (A) there is an ensemble of nine identical molecules, which are scattered about, in all possible orientations. It is anticipated that no fewer than 1000 micrographs, each with about 100 such molecules, will be needed to provide a complete data set. While a sufficiently large ensemble of molecules provides the full data needed to reconstruct a density map at high resolution, the challenge is to align their images and merge the data within a reasonable use of computational resources. In (B), however, the same ensemble of molecules has been prealigned by biochemical means (i.e., by crystallization of the sample). Merging the data is then done by computing the Fourier transform of the image. Such samples must still be tilted, however, in order to collect a three-dimensional data set. In practice a different crystal is used at each tilt angle.

THE ROLE OF CRYSTALS IN CRYSTALLOGRAPHY

For the sake of discussion we will assume that the only difference between an ensemble of molecules that is organized into a crystal and the same number of molecules when they are dispersed at random is the fact that the molecules in the crystal are prealigned, both translationally and in orientation (Fig. 2). In other words, we set aside, for the moment, any difference in conformation that may exist when molecules are in the dispersed state rather than in a crystal.

The only theoretical advantage of using well-ordered crystalline arrays (as in the work on bacteriorhodopsin, tubulin, etc.) then lies in the fact that merging data from statistically noisy images of crystals is computationally trivial, at least with modern computational power. A two-dimensional Fourier transform is all that is required, although additional computation ("unbending") is used in practice to correct imperfect long-range order in the alignment of individual protein molecules (Henderson *et al.,* 1986). A further practical advantage of having crystals comes from the fact that they can be used to obtain structure factor amplitudes from electron diffraction patterns. This latter point will

become less important as the experimental image contrast improves, ultimately approaching the situation in which the information content of an image is nearly the same as that in the scattered wave function. The minimum particle size that can be used to merge images of single molecules is likely to remain rather large, however, even as improvements are made in the image contrast. As a result, small ordered arrays, helixes, etc. will continue to be needed when the molecular weight of a protein is below a given limit.

The computational burden of aligning the images of 1 000 000 individual molecules (currently a typical value for high-resolution work that is based on 2-D crystals), or even 100 000 molecules (a figure that one may hope will ultimately become sufficient), is—in contrast—not yet a trivial one. A straw-man argument illustrates the problem. As pointed out by Henderson (1995), an exhaustive search over all possible ways to align projections of a reference particle to a single image could involve the calculation of 10^{14} cross-correlation functions. Each such cross-correlation function might involve 10^4 to 10^5 floating point operations (flops), depending upon the particle size. When done for 10^6 individual particles, the result would be that alignment would require approximately Avogadro's number of flops. Even if performed with a modern teraflop machine, such a calculation would require $\sim 10^{12}$ s ($\sim$32 000 years), give or take an order of magnitude or so.

This is intended to be a straw-man argument, however, since an exhaustive search over all possible translations and orientations is never carried out. Rather, the alignment is bootstrapped from low resolution, where alignment is computationally trivial, to increasingly higher resolution, where only the immediate neighborhood of the previously estimated alignment is explored. Reduction of the final, high-resolution search to as little as 0.1 of the full range in each of the five dimensions already gains a factor of 10^5 in the required number of flops, and even tighter prealignment, achieved at lower resolution, further improves the situation. The arrival of teraflop supercomputers thus makes it timely to consider the computational feasibility of high-resolution electron crystallography that is based upon images of isolated particles rather than images of prealigned assemblies (i.e., crystals).

If we accept for the sake of argument that computational alignment of individual particles can be made trivial, what would be the advantage of using single particles rather than crystalline samples? One answer is immediately obvious: the lengthy work of searching for conditions to crystallize the sample would no longer be necessary. Instead, alignment of particles would be done computationally (*in silico*) rather than biochemically; how much easier structural biology would be if this were the case! A further, practical consideration is that one would not have to tilt the sample in order to collect a 3-D data set. This is important at the moment because unknown factors—including imperfect specimen flatness and perhaps specimen charging—degrade the quality of images to an increasing extent as the tilt angle is increased. Finally, and with some optimism, one can imagine that automated particle identification would make it unnecessary to carry out extensive purification of the specimen, the final stage again being done *in silico* rather than at the bench.

As indicated above, we have assumed—up to this point—that all particles in suspension are structurally identical. To what extent will departures from that assumption limit the scope of structural studies by electron microscopy? (1) Surface loops are likely to be disordered in many cases. We know this to be the case from the fact that surface loops are often disordered even in crystals prepared for X-ray crystallography. Furthermore, loops that are ordered in one crystal form may be disordered—or differently ordered—in another crystal form, and loops seen to be ordered in an X-ray structure may be disordered in solution, as determined by NMR spectroscopy. It is actually informative to know whether surface loops are disordered or not, and in this sense new information can be derived from the use of single particles, which might be obscured in crystalline specimens. In any case, the number of residues involved in disordered surface loops is normally a small fraction of the total structure, and the increased amount of disorder to be expected in solution will not affect the ability to complete structural studies at high resolution. (2) Conformational flexibility about hinges between domains, or any form of short-range disorder in quaternary structure, is more likely to exist in isolated particles than in crystalline specimens. When heterogeneity of quaternary structure does occur, such as that reported for the ribosomal 30S subunit (Gabaschvili *et al.,* 1999), it will certainly preclude the merging of data to high resolution. Two approaches will be open to deal with such cases. In the first approach, applicable when there are only a small number of discrete quaternary structures, different particles should fall automatically into different classifications. Thus, while the computational burden will scale as the number of discrete conformational states that are accessible to the particle in solution, the benefit will be that one will ultimately visualize the whole set of intermediate conformational states that the particle can adopt, and not just the single one that is compatible with a particular crystallization condition. In the second approach, substrate analogs, ligands, inhibitors, and

even conformation-specific monoclonal antibodies can be used to restrict the quaternary structure to one or a few states, as sometimes must be done as part of the protocol for crystallization. The final conclusion, then, is that the problem of flexible quaternary structure should be no worse for high-resolution structural studies of single particles than it is for crystalline specimens.

To summarize, the role of crystals in electron crystallography is twofold. The first role has been to render trivial the otherwise difficult task of merging data from a large number of individual molecules. Ever increasing computational speeds can make this role obsolete. The second role is to produce objects of sufficiently large size that alignment is physically possible. This second role of crystals (or more correctly, ordered arrays) will remain an important one, but it can be hoped that further improvements in image quality will erode even the importance of this point by reducing the size of the smallest particle that can be successfully aligned to only a small factor times the physically limiting size, discussed above, that is determined by the elastic scattering cross section and by the effects of radiation damage.

TOMOGRAPHY

Tomography is defined here to be the method used to produce a three-dimensional density map, using data collected from only a single particle. This is, of course, the only approach that is possible for objects whose structure is so heterogeneous that averaging (merging) of data from more than one particle is precluded. On the other hand, nothing prevents the merging of tomographic data sets when the objects being investigated are, in fact, structurally identical.

Tomographic data acquisition would seem to be the ideal method for the investigation of subcellular structure, since complex assemblies can be visualized *in situ* and in the context of their surrounding molecular and chemical environment (Baumeister *et al.,* 1999). Specimen preparation artifacts may still be an issue, but these can be minimal when using rapid cryo-fixation and should be far less intrusive than those sometimes encountered during cell disruption and the isolation of single particles. Tomographic reconstruction of subcellular structure thus holds the potential to reveal conformational states that are important *in situ,* but which are not populated under *in vitro* conditions; precisely such a situation may explain apparent paradoxes in the crystallographic structures of myosin S1 ATPase (Dominguez *et al.,* 1998). Furthermore, important subunit interactions, which do not survive cell rupture and copurification or immunoprecipitation or which fail to show up on two-hybrid genetic screens, might be discovered. Conversely, interactions that are found to exist under *in vitro* conditions, or through two-hybrid screens, may be shown to be absent under *in vivo* conditions or to form in some local regions within the cell but not others. Tomographic structural biology thus holds the potential to tell us a great deal about functional genomics that crystallography, biochemistry, and molecular genetics themselves cannot provide.

Radiation damage of single particles again sets a limit as to how extensively such proposals can be realized. By confining our three-dimensional data collection to a single particle (or to a single field-of-view), tomographic reconstructions will be limited to ~2.8-nm resolution, i.e., to protein domains of ~17 kDa. The dose-fractionation theorem of tomography has once again been used to make this estimate. Even this estimate may be too conservative; as quoted by Henderson (1995), individual molecules of cytochrome C (MW 12 kDa) can already be seen experimentally in ice-embedded samples with electron exposures below 500 nm^{-2}, and further improvements in image quality are still likely to occur. As stated above, the same molecular mass could therefore be visualized in three-dimensional, tomographic reconstructions, simply by fractionating the same electron exposure over a suitably large number of tilted views of the sample. In this case, however, factors (perhaps charging) that progressively degrade the quality of images at high tilt angles must clearly be brought under control.

As fortune would have it, a resolution of ~2.5 nm is about the value at which accurate docking of previously determined, high-resolution structures can become highly informative. In addition, complex molecular assemblies can often be expected to occur in hundreds or even many thousands of identical copies within a single cell. In such cases their 3-D (tomographic) images can be merged, resulting in proportionately higher resolution representations of the structure. Thus, in favorable cases, hybrid crystallographic/tomographic structural biology of the cell holds considerable promise.

A major limitation on tomographic characterization of thick, cellular structures exists, which requires further work in the area of specimen preparation. Small microbial cells (Baumeister *et al.,* 1999) and the thin margins of cultured eukaryotic cells, both of which can be less than 500 nm thick, pose no problem since they can be prepared as whole-mount, frozen hydrated specimens. Thick eukaryotic cells and tissues, however, more representative of the real physiological condition, pose unresolved challenges for the preservation of molecular structure at a resolution that would be suitable for hybrid crystallography/tomography. Even if cryo-fixation could be achieved in thick specimens, by high-pressure freez-

ing as an example, methods for cutting adequate cryo-sections still remain elusive. Perhaps an earlier approach, involving the use of water-soluble polymer embedments (Langer *et al.,* 1975), may be worth reinvestigation. Specimen preparations that are comparable to embedment in aurothioglucose (Kuhlbrandt, 1982), metrizimide (Lepault *et al.,* 1983), or glucose-6-phosphate (Massover, 1998) would provide substantial contrast, yet might also be compatible with freeze-substitution and high-quality sectioning. Success in high-quality preservation of protein structure within sectionable tissue would again reinvigorate the nearly exhausted field of subcellular ultrastructure.

ANTICIPATING THE FUTURE

The physics of electron interaction with organic matter and the physics of image formation in the electron microscope both allow far more to be accomplished than is currently the case. Successes achieved with the use of two-dimensional crystals, while still fraught with experimental difficulty and requiring very considerable time for completion, have shown what is possible. Three-dimensional density maps have been obtained at high enough resolution to determine the atomic structure of proteins such as bacteriorhodopsin (Grigorieff *et al.,* 1996; Kimura *et al.,* 1997), a photosynthetic light-harvesting complex (Kuhlbrandt *et al.,* 1994), and tubulin (Nogales *et al.,* 1998). It is especially important to understand that quantitative measurements of the fall-off of structure factor amplitudes at high resolution (Baldwin *et al.,* 1988; Henderson, 1992) show that the image contrast at high resolution is typically 10% or less of what is could be. Major advances in the technical usefulness of electron crystallography would surely result if the high-resolution image contrast could be improved by as much as a factor of 3 or 4, thereby better approximating the information content of the scattered wave itself.

A first item on the agenda for the future thus needs to be to find a way to routinely bring the high-resolution image contrast to at least 35% of what it is in the scattered electron wave function. Improved methods to overcome the effects of specimen charging may still be needed, even though carbon coating (Jakubowski *et al.,* 1989; Brink *et al.,* 1998a), the use of a clean, gold objective aperture as a source of low-energy, secondary electrons, and taking care to uniformly illuminate the rim of carbon that surrounds the holes in which samples are embedded in vitreous ice (Brink *et al.,* 1998b) already do much to minimize the more obvious effects of charging. The use of field emission guns, with improved spatial coherence, and of higher accelerating voltages, which provide improved temporal coherence and a reduction in elastic-inelastic double scattering, appears also to be important. Nevertheless, the physical basis for the discrepancy between the information content of images and that of the scattered electron wave is still not properly accounted for, and until it is, it will be difficult to design instrumentation and research protocols that palliate the underlying causes.

The second item on the agenda could be to improve the quality of direct electronic read-out of high-resolution images. Direct electronic read-out will be essential for high-throughput structural biology by electron microscopy of single particles. A realistic design target might be to capture 1000 images in an 8-h period, i.e., approximately one image every 30 s, each containing ~100 particles. Exceptional stability of the cryo-stage, with a settling time of only a few seconds after movement of the specimen, is thus a major requirement. Furthermore, for high-throughput data acquisition to be practical, the read-out device should have a minimum of 2000 × 2000 pixels, and preferably 4000 × 4000 or more. The detector modulation transfer function at the Nyquist frequency must be virtually perfect, for example, within 5% of theoretical, and the detective quantum efficiency must also be nearly perfect, for example, 0.95. These design specifications do not place excessive demands upon current engineering technology, although the commercially supported solutions may at first seem expensive.

With improved image performance and high-speed data acquisition in place, attention will then turn to automation of data collection (Oostergetel *et al.,* 1998; Kisseberth *et al.,* 1999). The recent development of microfabricated support films, with identical, perfectly circular holes located at predictable positions (Ermantraut *et al.,* 1998), enormously simplifies the protocol that can be used to automate image acquisition. As a result, no significant technical or engineering difficulties need to be overcome before automated acquisition of single-particle images can be made a routine feature of any electron microscope.

The final item remaining on the agenda would be to develop strategies by which automated identification of particles (Lata *et al.,* 1995), alignment of their images, and merging of the data at high resolution are accomplished with approximately 10^{17} floating point operations or less. This figure represents a constraint that must currently be met in order to complete a structure determination within a reasonable use of computational resources.

There is still a large gap between the current status of electron crystallography and what is envisioned for the future. Nevertheless, the goal is clear: to prepare a single-specimen grid, initiate the data

acquisition process, and return a day later to find a three-dimensional density map at 0.3-nm resolution rotating on the computer terminal, waiting to be interpreted in terms of an atomic resolution structure of the molecule. If all of this sounds like 21st century technology, it soon will be.

APPENDIX

Published calculations of the bright-field image of a single atom (Chiu and Glaeser, 1975; Spence, 1981) can be used to estimate the minimum electron exposure that is needed to define the position of each atom in a protein with adequate statistical definition. Since the Rose equation (Rose, 1948, 1957, 1973; Glaeser, 1971) will be used to estimate the required electron exposure, the first step is to model the image as a uniform disk of diameter 0.3 nm and then estimate the resulting contrast. This will be done by integrating the image intensity of a calculated single-atom image and then redistributing the same image intensity uniformly over the disk.

Single-atom images have been calculated many times, but in most cases the authors have used optimistic estimates of lens aberrations in order to estimate the best image quality that physics and engineering might allow. The parameters used by Chiu and Glaeser (1975) correspond well to current instrumentation, however, and thus the image profile obtained in that work is used for our model calculation. The image intensity of a single atom can be reasonably well approximated as an inverted cone whose base has a diameter of 0.3 nm. The phase-contrast image intensity at the center of the atom is less than that of the surrounding intensity; in the case of a carbon atom the intensity at the center of the atom will be approximately 7% lower than the background (details are explained in the next paragraph), and thus the contrast of an equivalent, uniform disk would be approximately 2%. This is the value used in Eq. (2).

The image profile published by Chiu and Glaeser (1975), like most that have been published in the literature, is that of a heavy atom. However, the image profile of a carbon atom can be inferred from that of a heavy atom and the fact that the elastic scattering cross section for carbon is about four times smaller than that of a heavy atom. The phase-object contrast (which scales as the scattered amplitude rather than the scattering cross section) will thus be approximately half that of a heavy atom. The conclusion that the bright-field image contrast of a carbon atom is about half that of a heavy atom is further borne out by Fig. 6.9 in Spence (1981), which graphs the peak contrast as a function of atomic number. The absolute values of the contrast in that figure are, unfortunately, too optimistic for our present purpose because of the small value for spherical aberration that was assumed for the calculations. Since the peak image contrast of a mercury atom was calculated to be 14% (Chiu and Glaeser, 1975), we estimate that the peak value for a carbon atom would be 7%.

It is worth emphasizing that the real-space approach considered in this paper is based upon single-atom images in which the phase-contrast transfer function of the microscope is explicitly taken into account. Although only the image at Scherzer focus is considered, the poor contrast-transfer at low spatial frequency is fully represented. At the same time, the doubling in the magnitude of structure-factor amplitudes in the image intensity (relative to those in the scattered electron intensity), which occurs at the peak values of the contrast transfer function (Henderson and Glaeser, 1985), is also represented. The fact that only some of the scattered electrons (corresponding to a realistic resolution limit of about 0.3 nm) contribute useful signal to the image is automatically accounted for as well in the real-space approach.

I thank Dr. Joachim Frank and Dr. Richard Henderson for valuable comments on a preliminary draft, and I thank Dr. Kenneth Downing and Dr. Eva Nogales for participating in many discussions, which have refined my understanding of the topics covered in this paper. I also thank Dr. Bing Jap and Dr. Joachim Frank for emphasizing the importance of the dynamic flexibility of macromolecular structures. Dr. Michael Rossmann contributed the important reminder that the required number of projection directions, if not the number of particles, increases linearly with particle size. The work presented here was supported by NIH Grant GM 51487.

REFERENCES

Agrawal, R. K., Penczek, P., Grassucci, R. A., and Frank, J. (1998) Visualization of elongation factor G on the *Escherichia coli* 70S ribosome: The mechanism of translocation, *Proc. Natl. Acad. Sci. USA* **95,** 6134–6138.

Baldwin, J. M., Henderson, R., Beckman, E., and Zemlin, F. (1988) Images of purple membrane at 2.8Å resolution obtained by cryo-electron microscopy, *J. Mol. Biol.* **202,** 585–591.

Baumeister, W., Grimm, R., and Walz, V. (1999) Electron tomography of molecules and cells, *Trends Cell Biol.* **9,** 81–85.

Bottcher, B., Wynne, S. A., and Crowther, R. A. (1997) Determination of the fold of a core protein of hepatitis B virus by electron cryomicroscopy, *Nature* **386,** 88–91.

Breedlove, J. R., and Trammel, G. T. (1970) Molecular microscopy: Fundamental limitations, *Science* **170,** 1310–1313.

Brink, J., Gross, H., Tittmann, P., Sherman, M. B., and Chiu, W. (1998a) Reduction of charging in protein electron cryomicroscopy, *J. Microsc.* **191,** 67–73.

Brink, J., Sherman, M. B., Berriman, J., and Chiu, W. (1998b) Evaluation of charging on macromolecules in electron cryomicroscopy, *Ultramicroscopy* **72,** 41–52.

Caspar, D. L. (1975) Distinct images from invisible micrographs, *Nature* **257,** 9–10.

Chiu, W., and Glaeser, R. M. (1975) Single atom image contrast:

Conventional dark-field and bright-field electron microscopy, *J. Microsc.* **103,** 33–54.

Conway, J. F., Cheng, N., Zlotnick, A., Wingfield, P. T., Stahl, S. J., and Steven, A. C. (1997) Visualization of a 4-helix bundle in the hepatitis B virus capsid by cryo-electron microscopy, *Nature* **386,** 91–94.

Crowther, R. A., DeRosier, D. J., and Klug, A. (1970a) The reconstruction of a three-dimensional structure from projections and its application to electron microscopy, *Proc. R. Soc. London* **317,** 319–340.

Crowther, R. A., Amos, L. A., Finch, J. T., DeRosier, D. J., and Klug, A. (1970b) Three-dimensional reconstructions of spherical viruses by Fourier synthesis from electron micrographs, *Nature* **226,** 421–425.

DeRosier, D., and Klug, A. (1968) Reconstruction of 3-dimensional structures from electron micrographs, *Nature* **217,** 130–134.

Dominguez, R., Freyzon, Y., Trybus, K. M., and Cohen, C. (1998) Crystal structure of a vertebrate smooth muscle myosin motor domain and its complex with the essential light chain: Visualization of the pre-power stroke state, *Cell* **94,** 559–571.

Dubochet, J., Lepault, J., Freeman, R., Berriman, J. A., and Homo, J.-C. (1982) Electron microscopy of frozen water and aqueous suspensions, *J. Microsc.* **128,** 219–237.

Dubochet, J., Adrian, M., Chang, J. J., Homo, J.-C., Lepault, J., McDowall, A. W., and Schultz, P. (1988) Cryo-electron microscopy of vitrified specimens, *Quart. Rev. Biophys.* **21,** 129–228.

Ermantraut, E., Wohlfart, K., and Tichelaar, W. (1998) Perforated support foils with pre-determined hole size, shape and arrangement, *Ultramicroscopy* **74,** 75–81.

Frank, J. (1975) Averaging of low exposure electron micrographs of nonperiodic objects, *Ultramicroscopy* **1,** 159–162.

Frank, J. (1996) Three-Dimensional Electron Microscopy of Macromolecular Assemblies, Academic Press, San Diego.

Frank, J., and van Heel, M. (1982) Correspondence analysis of aligned images of biological particles, *J. Mol. Biol.* **161,** 134–137.

Frank, J., Chiu, W., and Degn, L. (1988) The characterization of structural variation within a crystal field, *Ultramicroscopy* **26,** 345–360.

Gabaschvili, I. S., Agrawal, R. K., Grassucci, R., and Frank, J. (1999) Structure and structural variations of the *Escherichia coli* 30S ribosomal subunit as revealed by three-dimensional cryo-electron microscopy, *J. Mol. Biol.* **286,** 1285–1291.

Glaeser, R. M. (1971) Limitations to significant information in biological electron microscopy as a result of radiation damage, *J. Ultrastruct. Res.* **36,** 466–482.

Glaeser, R. M., and Thomas, G. (1969) Application of electron diffraction to biological electron microscopy, *Biophys. J.* **9,** 1073–1099.

Glaeser, R. M., Cosslett, V. E., and Valdre, U. (1971a) Low temperature electron microscopy: Radiation damage in crystalline biological materials, *J. Microsc.* **12,** 133–138.

Glaeser, R. M., Kuo, I., and Budinger, T. (1971b) Method for processing of periodic images at reduced levels of electron radiation, *in* Proceedings of the 29th Annual Meeting of EMSA, pp. 466–467.

Grigorieff, N., Ceska, T. A., Downing, K. H., Baldwin, J. M., and Henderson, R. (1996) Electron-crystallographic refinement of the structure of bacteriorhodopsin, *J. Mol. Biol.* **259,** 393–421.

Hegerl, R., and Hoppe, W. (1976) Influence of electron noise on three-dimensional image reconstruction, *Z. Naturforsch.* **31a,** 1717–1721.

Henderson, R. (1992) Image contrast in high-resolution electron microscopy of biological macromolecules: TMV in ice, *Ultramicroscopy* **46,** 1–18.

Henderson, R. (1995) The potential and limitations of neutrons, electrons and X-rays for atomic resolution microscopy of unstained biological molecules, *Quart. Rev. Biophys.* **28,** 171–193.

Henderson, R., and Glaeser, R. M. (1985) Quantitative analysis of image contrast in electron micrographs of beam-sensitive crystals, *Ultramicroscopy* **16,** 139–150.

Henderson, R., Baldwin, J. M., Downing, K. H., Lepault, J., and Zemlin, F. (1986) Structure of purple membrane from *Halobacterium halobium:* Recording, measurement and evaluation of electron micrographs at 3.5A resolution, *Ultramicroscopy* **19,** 147–178.

Henderson, R., Baldwin, J. M., Ceska, T. A., Beckman, E., Zemlin, F., and Downing, K. (1990) A model for the structure of bacteriorhodopsin based on high resolution electron cryomicroscopy, *J. Mol. Biol.* **213,** 899–929.

Hoppe, W., Langer, R., Knesch, G., and Poppe, C. (1968) Protein-Krystallstrukturanalyse mit Elektronenstrahlen, *Naturwissenschaften* **55,** 333–336.

Hoppe, W., Gassmann, J., Hunsmann, N., Schramm, H. J., and Sturm, M. (1974) Three-dimensional reconstruction of individual negatively stained fatty-acid synthetase molecules from tilt series in the electron microscope, *Hoppe-Seyler Z. Physiol. Chem.* **355,** 1483–1487.

Jakubowski, U., Baumeister, W., and Glaeser, R. M. (1989) Evaporated carbon stabilizes thin, frozen-hydrated specimens, *Ultramicroscopy* **31,** 351–358.

Kimura, Y., Vassylyev, D. G., Miyazawa, A., Kidera, A., Matsushima, M., Mitsuoka, K., Murata, K., Hirai, T., and Fujiyoshi, Y. (1997) Surface of bacteriorhodopsin revealed by high-resolution electron crystallography, *Nature* **389,** 206–211.

Kisseberth, N., Brauer, G., Grosser, B., Potter, C. S., and Carragher, B. (1999) Java Scope: A web-based TEM control interface, *J. Struct. Biol.* **125,** 229–234.

Klug, A., and Berger, J. E. (1964) An optical method for the analysis of periodicities in electron micrographs, and some observations on the mechanism of negative staining, *J. Mol. Biol.* **10,** 565–569.

Knauer, V., Hegerl, R., and Hoppe, W. (1983) Three-dimensional reconstruction and averaging of 30S ribosomal subunits of *Escherichia coli* from electron micrographs, *J. Mol. Biol.* **163,** 409–430.

Krebs, A., Villa, C., Edwards, P. C., and Schertler, G. F. (1998) Characterization of an improved two-dimensional $p22_12_1$ crystal from bovine rhodopsin, *J. Mol. Biol.* **282,** 991–1003.

Kuhlbrandt, W. (1982) Discrimination of protein and nucleic acids by electron microscopy using contrast variation, *Ultramicroscopy* **7,** 221–232.

Kuhlbrandt, W., Wang, D. N., and Fujiyoshi, Y. (1994) Atomic model of plant light-harvesting complex by electron crystallography, *Nature* **367,** 614–621.

Kuo, I. A. M., and Glaeser, R. M. (1975) Development of methodology for low exposure, high resolution electron microscopy of biological specimens, *Ultramicroscopy* **1,** 53–66.

Labaw, L. W., and Rossmann, M. G. (1969) Electron microscopic observations of L-lactate dehydrogenase crystals, *J. Ultrastruct. Res.* **27,** 105–117.

Langer, R., Poppe, Ch., Schramm, H. J., and Hoppe, W. (1975) Electron microscopy of thin crystal sections, *J. Mol. Biol.* **93,** 159–165.

Lata, K. R., Penczek, P., and Frank, J. (1995) Automatic particle picking from electron micrographs, *Ultramicroscopy* **58,** 381–391.

Lepault, J., Booy, F. P., and Dubochet, J. (1983) Electron microscopy of frozen biological suspensions, *J. Microsc.* **129,** 89–102.

Levy, D., Mosser, G. M., Lambert, O., Moeck, G. S., Bald, D., and Rigaud, J.-L. 2-D crystallization of membrane proteins on lipid layer, in preparation.

Malhotra, A., Penczek, P., Agrawal, R. K., Gabaschvili, I. S., Grassucci, R. A., Junemann, R., Burkhardt, N., Nierhaus, K. H., and Frank, J. (1998) *Escherichia coli* 70S ribosome at 15Å resolution by cryo-electron microscopy: Localization of fmet-tRNAfMet and fitting of L1 protein, *J. Mol. Biol.* **280,** 103–116.

Marton, L. (1968) Early History of the Electron Microscope, San Francisco Press, San Francisco.

Massover, W. H. (1998) Glucose-6-phosphate is an unconventional negative stain, *in* Calderon Benavides, H. A., and Yacaman, M. J. (Eds.), Vol. 1, pp. 759–760, 14th ICEM, Inst. Physics Publishing, Philadelphia.

Matricardi, V. R., Moretz, R. C., and Parsons, D. F. (1972) Electron diffraction of wet proteins: Catalase, *Science* **177,** 268–270.

McEwen, B. F., Downing, K. H., and Glaeser, R. M. (1995) The relevance of dose-fractionation in tomography of radiation-sensitive specimens, *Ultramicroscopy* **60,** 357–373.

Mitsuoka, K., Murata, K., Walz, T., Hirai, T., Agre, P., Heymann, J. B., Engel, A., and Fujiyoshi, Y. (1999) The structure of aquaporin-1 at 4.5 Å resolution reveals short α-helices in the center of the monomer, *J. Struct. Biol.* **128**, 34–43.

Miyazawa, A., Fujiyoshi, Y., Stowell, M., and Unwin, N. (1999) Nicotinic acetylcholine receptor at 4.6Å resolution: Transverse tunnels in the channel wall, *J. Mol. Biol.* **288,** 765–786.

Nogales, E., Wolf, S. G., and Downing, K. H. (1998) Structure of the tubulin dimer by electron crystallography, *Nature* **391,** 199–203.

Nogales, E., Whittaker, M., Milligan, R. A., and Downing, K. H. (1999) High resolution model of the microtubule, *Cell* **96,** 79–88.

Oettl, H., Hegerl, R., and Hoppe, W. (1983) Three-dimensional reconstruction and averaging of 50S ribosomal subunits of *Escherichia coli* from electron micrographs, *J. Mol. Biol.* **163,** 431–450.

Olson, N. H., Kolatkar, P. R., Oliveira, M. A., Cheng, R. H., Greve, J. M., McClelland, A., Baker, T. S., and Rossmann, M. G. (1993) Structure of a human rhinovirus complexed with its receptor molecule, *Proc. Natl. Acad. Sci. USA* **90,** 507–511.

Oostergetel, G. T., Keegstra, W., and Brisson, A. (1998) Automation of specimen selection and data acquisition for protein electron crystallography, *Ultramicroscopy* **74,** 47–59.

Parsons, D. F., and Martius, U. (1964) Determination of the α-helix configuration of poly-γ-benzyl-L-glutamate by electron diffraction, *J. Mol. Biol.* **10,** 530–533.

Rayment, I., Holden, H., Whittaker, M., Yohn, C., Lorenz, M., Holmes, K., and Milligan, R. (1993) Structure of the actin–myosin complex and its implications for muscle contraction, *Science* **261,** 58–65.

Rose, A. (1948) Television camera tubes and the problem of vision, *Adv. Electronics Electron Phys.* **1,** 131–166.

Rose, A. (1957) Quantum effects in human vision, *Adv. Biol. Med. Phys.* **5,** 211–242.

Rose, A. (1973) Vision: Human and Electronic, Plenum, New York.

Saxberg, B. E. H., and Saxton, W. O. (1981) Quantum noise in 2D projections and 3D reconstructions, *Ultramicroscopy* **6,** 85–90.

Saxton, W. O., and Frank, J. (1977) Motif detection in quantum noise-limited electron micrographs by cross-correlation, *Ultramicroscopy* **2,** 219–227.

Spence, J. C. H. (1981) Single atoms in bright field, *in* Experimental High-Resolution Electron Microscopy, Sect. 6.2, pp. 197–216, Clarendon, Oxford.

Taylor, K. A., and Glaeser, R. M. (1974) Electron diffraction of frozen, hydrated protein crystals, *Science* **186,** 1036–1037.

Unger, V. M., Kumar, N. M., Gilula, N. B., and Yeager, M. (1999) Three-dimensional structure of a recombinant gap junction membrane channel, *Science* **283,** 1176–1180.

Unwin, P. N. T., and Henderson, R. (1975) Molecular structure determination by electron microscopy of unstained crystalline specimens, *J. Mol. Biol.* **94,** 425–440.

van Heel, M., and Frank, J. (1981) Use of multivariate statistical statistics in analyzing the images of biological macromolecules, *Ultramicroscopy* **6,** 187–194.

Wilson-Kubalek, E. M., Brown, R. E., Celia, H., and Milligan, R. (1998) Lipid nanotubes as substrates for helical crystallization of macromolecules, *Proc. Natl. Acad. Sci. USA* **95,** 8040–8045.

Zhang, P., Toyoshima, C., Yonekura, K., Green, N. M., and Stokes, D. L. (1998) Structure of the calcium pump from sarcoplasmic reticulum at 8Å resolution, *Nature* **392,** 835–839.